

# Analytical Methods

Accepted Manuscript



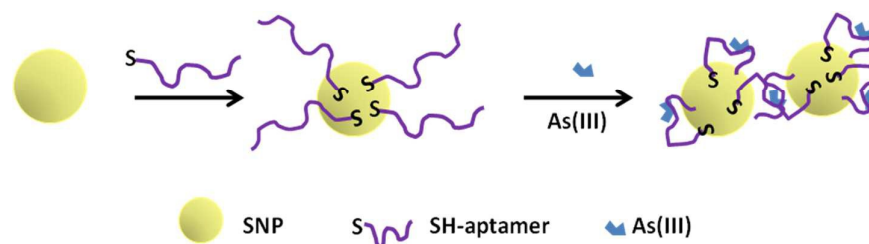
This is an *Accepted Manuscript*, which has been through the Royal Society of Chemistry peer review process and has been accepted for publication.

*Accepted Manuscripts* are published online shortly after acceptance, before technical editing, formatting and proof reading. Using this free service, authors can make their results available to the community, in citable form, before we publish the edited article. We will replace this *Accepted Manuscript* with the edited and formatted *Advance Article* as soon as it is available.

You can find more information about *Accepted Manuscripts* in the [Information for Authors](#).

Please note that technical editing may introduce minor changes to the text and/or graphics, which may alter content. The journal's standard [Terms & Conditions](#) and the [Ethical guidelines](#) still apply. In no event shall the Royal Society of Chemistry be held responsible for any errors or omissions in this *Accepted Manuscript* or any consequences arising from the use of any information it contains.

1  
2  
3 Aptamer conjugated silver nanoparticles were synthesized for the colorimetric detection of  
4  
5 As(III) ions in solution. The central composite design combined with response surface  
6  
7 methodology was employed to maximize the efficiency of sensing.  
8  
9  
10



Cite this: DOI: 10.1039/c0xx00000x

www.rsc.org/xxxxxx

ARTICLE TYPE

# Aptamer conjugated silver nanoparticles for the colorimetric detection of arsenic ions using response surface methodology

Faten Divsar,<sup>a\*</sup> Kazhal Habibzadeh,<sup>b</sup> Shahab Shariati<sup>b</sup> and Mehdi Shahriarinnour<sup>c</sup>*Received (in XXX, XXX) Xth XXXXXXXXXX 20XX, Accepted Xth XXXXXXXXXX 20XX*

DOI: 10.1039/b000000x

In this study, aptamer conjugated silver nanoparticles (Apt-SNPs) were synthesized and studied for colorimetric sensing of As (III) ions in solution. As (III) ions specifically interact with Apt-SNPs to form As (III)-Apt-SNPs and cause a remarkable decrease in absorbance peak of silver nanoparticles at 403 nm, which enables the determination of As (III) with high selectivity and sensitivity. A three-factor, central composite design (CCD) optimization method combined with response surface methodology (RSM) was employed to maximize the efficiency of arsenic detection. The significance of the independent variables and their interactions were tested using the analysis of variance (ANOVA). The linear dynamic range of the colorimetric Apt-SNPs based optical sensor covered a large variation of As (III) concentration from 50 to 700  $\mu\text{g L}^{-1}$  and the detection limit of 6  $\mu\text{g L}^{-1}$  was obtained. Moreover, this assay was able to detect As (III) ions with high sensitivity and revealed to have remarkable potential applications.

## Introduction

Arsenic contamination of drinking and ground waters is turning out to be a serious worldwide threat to human health<sup>1</sup>. Arsenic is a naturally occurring element which is found in soil and water resources<sup>2,3</sup>. Arsenic concentrations vary in accordance with geographic location. When arsenic levels are found to be too high in a specific location, it may be necessary to detect and remove it from drinking water. Arsenic usually exists in two different forms depending on the amount of oxygen content of water. In deeper, anaerobic ground waters, arsenic usually occurs as arsenite, As (III), which is 60 times more toxic than As (V) or organic arsenic compounds<sup>4</sup>. Drinking water contaminated with As (III) is associated with a number of diseases such as skin damage or problems with circulatory systems, and high risk of getting cancer<sup>1</sup>. Currently, the popular methods for arsenic detection are chromatography, spectroscopic and electrochemistry methods<sup>5</sup>. These techniques are well established but require complicated instrumentation which is demanding, expensive and require significant maintenance and operator expertise.

Aptamers are single-stranded RNA or DNA oligonucleotides with noticeable affinity to their specific targets. This characteristic of aptamers is comparable to antibody-antigen interaction. Aptamers are selected by an in vitro process called SELEX. This process leads to the selection of high affinity sequences to a special target. Since aptamers are high affinity selective-acting compounds, they have lots of applications in different fields of science<sup>6</sup>. Indeed, the past few years have witnessed a variety of aptasensors in the aspects of electrochemical, surface-enhanced Raman scattering, fluorescent and colorimetric assays<sup>7-14</sup>. However, only a few reports have addressed these issues in the context of colorimetric aptasensor for metal ions<sup>15,16</sup>. Among the developed aptamer-based nanosensors, metallic NPs such as gold nanoparticles (AuNPs) and silver nanoparticles (SNPs) are the most common. Metallic NPs that have strongly distance-dependent optical properties and

large surface areas have emerged as important colorimetric materials<sup>17</sup>. Some aptasensors for the detection of several metal ions, including  $\text{Pb}^{2+}$ ,  $\text{Hg}^{2+}$ ,  $\text{K}^{+}$  and  $\text{As}^{3+}$  have been reported<sup>18-21</sup>.

Whereas SNPs have surface plasmon peak at about 400 nm with high extinction coefficients and excellent optical properties, we herein developed a colorimetric sensor based on aptamer conjugated silver nanoparticles (Apt-SNPs) employing the structure switching aptamer for As (III) ions detection.

Central composite design (CCD) based response surface methodology (RSM) which is a compilation of statistical techniques for designing experiments, building models, evaluating the effects of factors and searching for the optimum conditions, has successfully been used for optimizing various experimental parameters.

## Experimental

### Materials and instruments

Silver nitrate, sodium borohydride, potassium chloride, potassium hydroxide, sodium dihydrogen phosphate, disodium hydrogen phosphate, poly vinyl pyrrolidone, nitric acid and hydrochloric acid with analytical reagent grade were purchased from commercial sources (Merck or Sigma-Aldrich). The aqueous solution of As (III) ( $1000 \text{ mg L}^{-1}$ ) was prepared and used as a stock solution. Thiolated arsenic-binding aptamer<sup>21</sup> with the following sequence was obtained from NedayeFan Co. (Tehran, Iran):

5'-HS-GGTAATACGACTCACTATAGGGAGATACCAGCT TATTCAATTTTACAGAACAACCAACGTCGCTCCGGGTACTTCTTCATCGAGATAGTAAGTGCAATCT-3'

The stock solution of the aptamer ( $40 \text{ mg L}^{-1}$ ) was prepared using phosphate buffer solution (PBS) ( $\text{pH}=7.4$ ) and kept at  $-20 \text{ }^\circ\text{C}$ . All experiments were performed at room temperature and double distilled water was used in all solution preparations.

Scanning electron microscope (SEM) observations were carried out with a Phillips XL-30 microscope (Netherlands). UV-Vis absorption spectra were recorded on a Hach DR5000 UV-Vis Spectrophotometer (USA). A Hettich centrifuge model universal 320R (Germany) was applied to accelerate the separation process. A Hach Sension 378 pH meter (USA) with a combined glass electrode was used for pH measurements.

### Synthesis of aptamer-conjugated silver nanoparticles (Apt-SNPs)

All the glassware used in the procedure was first dipped in aqua regia (HNO<sub>3</sub>/HCl, 1:3), then washed thoroughly with double distilled water and dried in an oven. SNPs were prepared according to a procedure previously reported in the literature<sup>22</sup>. Briefly, an excess amount of sodium borohydride is needed both for chemical reduction of the ionic silver and to stabilize the silver nanoparticles. The sodium borohydride was chilled to roughly 0 °C using ice during stirring. A 2.0 mL aliquot of silver nitrate (1.0 mM) was added drop by drop (~1 drop/s) to 30.0 mL of 3.0 mM sodium borohydride solution at 0 °C. The reaction mixture was stirred vigorously on a magnetic stirrer. The solution turned to light yellow after the addition of 2.0 mL of silver nitrate. The colloid was continuously stirred while it was allowed to warm to room temperature. In order to minimize the aggregation of SNPs, 1 mL of 0.3% (w/v) polyvinylpyrrolidone (PVP) was then added to the resulting solution. Synthesized SNPs could be stored in a dark bottle (4 °C) for several days. Then, 20 μL of 1 mg L<sup>-1</sup> deprotected aptamer was added to SNPs solution and kept for 18 h for the strong covalently bonding of thiol group of aptamer segments to SNPs.

The free aptamers were removed by centrifuge and the Apt-SNPs were redispersed in 2 mL phosphate buffer solution (PBS) (pH = 7.4).

### Colorimetric detection of As (III)

A series of different concentrations of As (III) ions ranging from 50 to 700 μg L<sup>-1</sup> in the Apt-SNPs solution (2 mL) was made. After carefully mixing in the sonicator for a few seconds, the mixture was centrifuged and the As(III)-Apt-SNPs were redispersed in 2 mL PBS buffer (pH = 7.4). The resulting solutions were transferred to a 1-cm quartz cuvette and the spectral changes were observed by UV-Vis spectrophotometer. The absorbance spectra ranging from 200 to 700 nm was recorded for each sample to indicate the aggregation of the SNPs. All assays were performed at room temperature.

### Optimization of experimental conditions

The design and analysis of experiments were performed using design expert software (version 6.0.6, Stat-Ease, Inc., Minneapolis, MN, USA). After detecting the respective working ranges of the variables, the central composite design (CCD) based response surface methodology (RSM) was applied for the optimization of the main experimental parameters such as the concentration of aptamer (A), conjugation time (B) and pH (C). All factors were controlled at five levels. This design was based on a 2<sup>3</sup> factorial design, six replicates of the central run, leading to 20 sets of experiments, enabling each experimental response to be optimized. The standard RSM was selected for the optimization of the factors which affected the assay response. CCD consisted of three levels coded as -1, 0, 1 and two alpha levels coded as (±)1.68. The actual values with respect to coded values of each factor are shown in Table 1.

The response variable (Y) that represented the absorbance or concentration of As (III) was fitted by a second-order model in the form of quadratic polynomial equation:

$$Y = a_0 + \sum_{i=1}^3 a_i X_i + \sum_{i=1}^3 a_{ii} X_i^2 + \sum_{i=1}^2 \sum_{j=i+1}^3 a_{ij} X_i X_j$$

Where Y is the predicted response variable, a<sub>0</sub>, a<sub>i</sub>, a<sub>ii</sub> and a<sub>ij</sub> are regression coefficients of the model, X<sub>i</sub> and X<sub>j</sub> represent the independent variables in the form of actual value.

RSM was a combination of experimental, regression analysis and statistical inferences. RSM not only reduced the cost and time, but also provided required information about the interaction effects with minimum number of experiments. Analysis of variance (ANOVA) was also utilized to test the significance of each term in the equation and the goodness of fit of the obtained regression model. Two-dimensional counter plots and three-dimensional curves of the response surface were also developed.

## Results and discussion

In the first step of the study, the range of operational variables, i.e., the concentration of aptamer, conjugation time, and pH on colorimetric detection of arsenic was investigated. In the second step, response surface methodology was used in order to achieve the main objective and optimal condition for detection of As (III) in solution.

### Preparation and spectrophotometric characterization of SNPs

The synthesized colloidal SNPs were identified by typical strong plasmon resonance band at 403 nm (Fig. 1a). To assay for As (III) ions, the thiolated aptamers were conjugated to SNPs separately via the strong Ag-S bond. The procedure keeps the aptamers upright on the surface of SNPs<sup>23,24</sup>. In the absence of As (III), the aptamer modified SNPs dispersed well in the solution and resulted no change in the UV-Vis absorption spectra (Fig. 1b). The size of the Apt-SNPs was verified through transmission electron microscope (TEM) analysis. It showed that the 12±3 nm SNPs are spherical and evenly distributed (Fig. 2a). As (III) ions could specifically bind to the aptamer and induced the Apt-SNPs switching from a well dispersed state to an aggregated one, resulting in a change in the UV-Vis absorption spectra of the solution (Fig. 1c). In this case, As (III) ions coordinate the phosphate and amine groups of the bases in DNA aptamers, which in turn cause the aggregation of aptamer conjugated silver nanoparticles (Fig. 2b). During the interaction, the aptamer formed a G-quadruplex structure, as shown in Scheme 1.

The influence of the amount of SNPs on the absorbance was investigated in the range of 0.1–1.0 mM of silver ions concentration. The absorbance increased up to a maximum when 1.0 mM of silver ions concentration was used; higher concentrations did not increase the signals significantly for 3.0 mM sodium borohydride concentration. So, 1.0 mM of silver ions concentration was chosen as optimum value.

### Effect of conjugation time

Incubation studies were done to determine the stability of aptamer after conjugating with the SNPs at different time periods at room temperature. As shown in Fig. 3, from the results of UV-Vis spectra obtained at different conjugation times, 18 h made maximum absorbance difference in spectra after the addition of As (III) ions. It raised from sufficient reaction time which was given to the aptamers to bind to SNPs before using for As (III)

ions sensing. Thus, among all of the incubation times, 18 h was selected as the optimal time.

### Effect of pH and time on the stability of Apt-SNPs

Fig. 4a shows the effect of pH on the stability of synthesized Apt-SNPs. From the figure, we can observe that the newly synthesized nanoparticles are extremely stable when pH is about 7.4. Under this biological pH condition, the synthetic Apt-SNPs were quite stable probably due to strong interparticle electrostatic repulsion between the negatively-charged aptamer probes on the nanoparticles surface. Fig. 4b shows the absorption spectra of Apt-SNPs recorded at different times. For Apt-SNPs, there was no obvious change in the shape, position and symmetry of the absorption peak during 3 hours, showing the stability of synthesized Apt-SNPs.

### Effect of the aptamer concentration

In this assay, the concentration of aptamers in the range of 0.5-10 mg L<sup>-1</sup> was investigated to obtain the best amount of aptamer needed for detection of As (III) ions (Fig. 5). The figure shows that the aptamer concentration of 1 mg L<sup>-1</sup> is sufficient to bind with constant amount of As (III), resulting in more As (III)-induced aggregation, whereas lower concentrations of aptamers were not completely sufficient for binding to the arsenic ions. In contrast, at higher concentrations, excessive aptamers acted as electrostatic barriers. Thus, 1 mg L<sup>-1</sup> aptamer concentration was chosen as optimum amount for further studies.

### Fabrication of colorimetric sensor for determination of As (III) ions

To detect As (III) ions using the SNP-based colorimetric aptasensor, UV-Vis spectra of Apt-SNPs were recorded with different concentrations of As (III) under the optimized experimental conditions (Fig. 6a). The resultant graph shows that the control, containing only Apt-SNPs, had higher absorbance as compared with Apt-SNPs with different concentrations of As (III) ions. The absorbance values at 403 nm decreased with the addition of As (III) so at higher concentration lowest absorbance value was observed. A very good linear relationship was observed between (A0-A)403 and the concentration of As (III) ions in solution, with a correlation coefficient (R<sup>2</sup>) of 0.992 in the range of 50 - 700 µg L<sup>-1</sup> (Fig. 6b) and a detection limit of 6 µg L<sup>-1</sup>. The relative standard deviations indicated that the proposed method offers excellent reproducibility (RSD=1.43%, n = 3). In addition, to show the advantages of proposed sensor, a comparison of the performance of proposed sensor with different metal ions aptasensors is shown in Table 2. From this Table, it can be seen that the detection limit of proposed sensor (6 µg L<sup>-1</sup>) is better than other aptasensors.

### Selectivity for detecting target As (III) ions

In order to evaluate the selectivity of the proposed sensor for the detection of As (III) ions, comparative trials were carried out using Na<sup>+</sup>, Ca<sup>2+</sup>, Cd<sup>2+</sup>, Pb<sup>2+</sup>, Sb<sup>3+</sup>, Bi<sup>3+</sup> and As (V) as the potential interference ions. As shown in Fig. 7a, the absorbance peaks of UV-Vis spectra for the mixture of the different metal ions other than As (III) ions had a little change compared with the background due to the low binding affinity of the Apt-SNPs to these ions and little tendency to form a G-quadruplex. However, upon the addition of 350 µg L<sup>-1</sup> As (III) ions, there was a noticeable change in UV-Vis adsorption spectra. In Fig. 7b, the value at the y-axis could be normalized by the absorbance peak decrease for As (III) versus background. The relative values of absorbance decrease (relative signal (%)) = (A403, SNPs - A403,

metal ions)/(A403, SNPs - A403, As(III)) were detected to be in the range of 11.7-38.7%. These results demonstrated that all other metal ions display slight and negligible interferences. Thus, the proposed method showed good selectivity for As (III) detection.

## Response surface methodology

### Experimental design and regression model

The individual and interactive effects of the experimental variables on the colorimetric detection of As (III) ions by the developed aptasensor in aqueous medium were investigated using the CCD approach. A three-factor model was selected for developing the mathematical relationship between the response and the process variables including aptamer concentration, conjugation time and pH. The range and level of experimental variables investigated in this study are shown in Table 1. The CCD based experiments to obtain a three-factor model consisted of 20 standard factorial runs, a star configuration ( $\alpha = \pm 1.68$ ) of size, and six replicates at the central point were used to determine the experimental error. The measured absorbance of the developed aptasensor corresponding to different combinations of selected experimental variables is presented in Table 3. A polynomial regression modeling was performed between the response variable (absorbance value) and the corresponding coded values (aptamer concentration (A), conjugation time (B) and pH (C)) and finally, the best fitted model equation was obtained as:  $Y = 0.66 + 0.065C - 0.12C^2$ .

### Effects of model components and their interactions on As (III) detection

The parameter effect is estimated as twice the regression coefficient value for that parameter. The p-value is used as a tool to check the significance of the coefficient. The larger the magnitude of the F-value and the smaller the p-value, the more significant is the corresponding parameter in the regression model<sup>29</sup>. From Table 4, it is evident that the linear and quadratic term are statistically significant ( $P < 0.0001$ ), whereas none of the interactive terms is significant. The statistical results (Table 4) further suggested that the pH of solution is among the process variables exhibiting the most significant effect on the detection process. Moreover, its respective quadratic effect (C<sup>2</sup>) was found to be relatively significant. The F- and p-values suggest that the pH of solution has a direct relationship on the As (III) detection efficiency of the developed aptasensor. It may be noted that the solution pH was the most significant component of the regression model for the present application.

### Model validation

The goodness of fit of the model was checked by the correlation coefficient (R<sup>2</sup>) between the experimental and model predicted values of the response variable (Fig. 8). A fairly high value of R<sup>2</sup> (0.97) indicated a high dependence and correlation between the measured and the predicted values of response. Moreover, a closely high value of the adjusted correlation coefficient (R<sup>2</sup> adj = 0.94) also showed a high significance of the model and that the total variation of about 94% for absorbance value was attributed to the independent variables and only about 6% of the total variation could not be explained by the model. The R<sup>2</sup> adj corrects the R<sup>2</sup> value for the sample size and the number of terms in the model. If there are many terms in the model and the sample size is not very large, the R<sup>2</sup> adj may be noticeably smaller than the R<sup>2</sup>. In our case, the values of R<sup>2</sup> adj and R<sup>2</sup> were found to be close.

### Three-dimensional response surface plots

The three-dimensional (3D) response surface plots of the dependent variables varying within their experimental ranges can be helpful in understanding both the main and the interaction effects of these independent variables. Therefore, in order to gain better understanding of the effects of the independent variables and their interactions on the dependent variable, 3D response surface plots for the measured responses were constructed based on the quadratic model. Since the quadratic model in this study had three independent variables, one variable was held constant at its center level for each plot and subsequently, a total of three 3D plots was formed for the responses.

The influence of three different variables on the absorbance value of developed aptasensor is visualized in the 3D response surface plots and their corresponding contour plots (Fig. 9a–c). Fig. 9a shows the three-dimensional response surface plot for absorbance value of the aptasensor as a function of aptamer concentration and conjugation time at constant solution pH. The absorbance value increases with conjugation time within its respective experimental range, whereas it declines with increasing aptamer concentration more than 1 mg L<sup>-1</sup>. The interactive effect of pH and aptamer concentration on the absorbance value of aptasensor at constant conjugation time is shown in Fig. 9b. It is evident that absorbance value decreases with aptamer concentration more than 1 mg L<sup>-1</sup> in the experimental range. Also, pH is an important parameter in the analytical experiments. The obtained data show that the aptasensor works accurately only at 7.0 to 8.0 pH ranges. This phenomenon may have occurred by the influence of pH not only on the aptamer-arsenic complex formation but also on the aptamer folding.

The combined effect of conjugation time and pH of the solution on absorbance value of the developed aptasensor at constant aptamer concentration (1 mg L<sup>-1</sup>) is shown in Fig. 9c. It can be noted that the absorbance value increases with conjugation time, while with moving away from pH 7.4, a decline was obtained. A maximum absorbance value of the developed aptasensor is observed at aptamer concentration 1 mg L<sup>-1</sup>, conjugation time 18 h and pH 7.0–8.0.

### Real sample analysis

In order to evaluate the performance of the proposed colorimetric sensor for detection of As (III) in real environmental matrices, river, well and tap water samples were analyzed. The absorbance value for tap, river and well waters were noted to be 0.456±0.1, 0.401±0.1 and 0.209±0.1 which correlates within the concentration range of 50.0, 93.5 and 669.2 µg L<sup>-1</sup> respectively. The concentration of arsenic in the real samples was also analyzed using a reference method, namely graphite furnace atomic absorption spectrometry (GF-AAS). Using GF-AAS, the arsenic concentrations in the tap, river and well waters were noted to be 50.1, 99.8 and 694.8 µg L<sup>-1</sup> respectively, validating quite well the performance of our newly developed method. The recovery levels of 96.8, 93.7 and 96.3 % in tap, river and well waters confirmed the effectiveness of this method for determination of As (III) ions. This also corroborates well with the literature reports of range of As (III) concentrations in the natural water matrices<sup>30,31</sup>.

### Conclusions

We successfully developed a colorimetric sensor with high sensitivity and specificity for detection of As (III) ions. The design is based on the aggregation of Apt-SNPs by As (III) ions.

Because As (III) has two binding sites for its aptamer, it can act as a bridge to link the monodispersed Apt-SNPs together. The method demonstrated a linear relationship from 50 to 750 µg L<sup>-1</sup> of As (III), with a detection limit of 6 µg L<sup>-1</sup>. A three-factor, central composite design (CCD) combined with response surface modeling (RSM) was employed for maximizing the colorimetric detection of As (III) ions. The proposed mathematical approach also provided a critical analysis of the individual and simultaneous interactive influences of the selected independent process variables, such as aptamer concentration (A), conjugation time (B) and pH (C) on As (III) detection by developed aptasensor. The optimal variables were optimally set as follows: aptamer concentration 1 mg L<sup>-1</sup>, conjugation time 18 h and pH 7.4.

The fit model was checked by correlation coefficient ( $R^2 = 0.97$ ) for the obtained quadratic model. The high correlation between the experimental response value and the response value predicted by the statistical model indicated the reliability of the proposed method.

The validation results clearly confirmed that the proposed three-factor CCD combined with RSM is an effective approach for modeling the colorimetric detection of As (III) ions using aptasensor in aqueous media.

### Notes and references

- <sup>a</sup> Department of Chemistry, Payame Noor University, Tehran, Iran. Fax: +98 131 6666427; Tel: +98 131 6606008; E-mail: f.divsar@gilan.pnu.ac.ir
- <sup>b</sup> Department of Chemistry, Rasht Branch, Islamic Azad University, Rasht, Iran.
- <sup>c</sup> Department of Microbiology, Rasht Branch, Islamic Azad University, Rasht, Iran
- M. Berg, H. C. Tran, T. C. Nguyen, H. V. Pham, R. Schertenleib and W. Giger, *Environ. Sci. Technol.*, 2001, **35**, 2621–2626.
  - S. Hu, J. Lu and C. Jing, *J. Environ. Sci.*, 2012, **24**, 1341–1346.
  - E. S. Forzani, K. Foley, P. Westerhoff and N. Tao, *Sens. Actuators, B*, 2007, **123**, 82–88.
  - B. K. Jena and C. R. Raj, *Anal. Chem.*, 2008, **80**, 4836–4844.
  - D. E. Mays and A. Hussam, *Anal. Chim. Acta*, 2009, **646**, 6–16.
  - L. Kashеfi-Kheyrabadi and M. A. Mehrgardi, *Biosens. Bioelectron.*, 2012, **37**, 94–98.
  - M. E. Stewart, C. R. Anderton, L. B. Thompson, J. Maria, S. K. Gray, J. A. Rogers and R. G. Nuzzo, *Chem. Rev.*, 2008, **108**, 494–521.
  - Z. Wang and Y. Lu, *J. Mater. Chem.*, 2009, **19**, 1788–1798.
  - Y. Lu and J. Liu, *Curr. Opin. Biotechnol.*, 2006, **17**, 580–588.
  - J. O. Lee, H. M. So, E. K. Jeon, H. Chang, K. Won and Y. H. Kim, *Anal. Bioanal. Chem.*, 2008, **390**, 1023–1032.
  - J. Jeon, D. K. Lim and J. M. Nam, *J. Mater. Chem.*, 2009, **19**, 2107–2117.
  - Y. F. Huang, K. M. Huang and H. T. Chang, *J. Colloid Interface Sci.*, 2006, **301**, 145–154.
  - Y. F. Huang, Y. W. Lin and H. T. Chang, *Nanotechnology*, 2006, **17**, 4885–4894.
  - C. D. Medley, J. E. Smith, Z. Tang, Y. Wu, S. Bamrungsap and W. Tan, *Anal. Chem.*, 2008, **80**, 1067–1072.
  - W. Zhao, W. Chiunan, J.C.F. Lam, S.A. McManus, W. Chen, Y. Cui, R. Pelton, M.A. Brook and Y. Li, *J. Am. Chem. Soc.*, 2008, **130**, 3610–3618.
  - S.J. Chen, Y.F. Huang, C.C. Huang, K.H. Lee, Z.H. Lin, H.T. Chang, *Biosens. Bioelectron.*, 2008, **23**, 1749–1753.
  - C. Burda, X. Chen, R. Narayanan and M. A. El-Sayed, *Chem. Rev.*, 2005, **105**, 1025–1102.
  - J. S. Lee, M. S. Han and C. A. Mirkin, *Angew. Chem. Int. Ed.*, 2007, **46**, 4093–4096.
  - L. Wang, X. Liu, X. Hu, S. Song and C. Fan, *Chem. Commun.*, 2006, **36**, 3780–3782.
  - Z. Wang, J. H. Lee and Y. Lu, *Adv. Mater.*, 2008, **20**, 3263–3267.

- 1  
2  
3  
4  
5  
6  
7  
8  
9  
10  
11  
12  
13  
14  
15  
16  
17  
18  
19  
20  
21  
22  
23  
24  
25  
26  
27  
28  
29  
30  
31  
32  
33  
34  
35  
36  
37  
38  
39  
40  
41  
42  
43  
44  
45  
46  
47  
48  
49  
50  
51  
52  
53  
54  
55  
56  
57  
58  
59  
60
- 21 Y. Wu, S. Zhan, F. Wang, L. He, W. Zhi and P. Zhou, *Chem. Commun.*, 2012, **48**, 4459–4461.
- 22 L. Mulfinger, S. D. Solomon, M. Bahadory, A. V. Jeyarajasingam, S. A. Rutkowsky and C. Boritz, *J. Chem. Educ.*, 2007, **84**, 322–325.
- 5 23 C. C. Huang, Y. F. Huang, Z. Cao, W. Tan, and H. T. Chang, *Anal. Chem.*, 2005, **77**, 5735–5741.
- 24 J. H. Oh and J. S. Lee, *Anal. Chem.*, 2011, **83**, 7364–7370.
- 25 J. Liu and Y. Lu, *J. Am. Chem. Soc.*, 2004, **126**, 12298–12305.
- 26 H. Wang, Y. Wang, J. Jin and R. Yang, *Anal. Chem.*, 2008, **80**, 9021–9028.
- 10
- 27 C. H. Chung, J. H. Kim, J. Juyeon and B. H. Chung, *Biosens. Bioelectron.*, 2013, **41**, 827–832.
- 28 A. Ravindran, M. Elavarasi, T. C. Prathna, A. M. Raichur, N. Chandrasekaran and A. Mukherjee, *Sens. Actuators B*, 2012, **166**, 365–371.
- 15
- 29 H. Meng, X. Hu and A. Neville, *Wear*, 2007, **263**, 355–362.
- 30 Z. Sharifi and A. A. Sinegani, *Curr. World Environ.*, 2012, **7**, 233–241.
- 31 S. Zandsalimi, N. Karimi and A. Kohandel, *Int. J. Environ. Sci. Tech.*, 2011, **8**, 331–338.
- 20

Cite this: DOI: 10.1039/c0xx00000x

www.rsc.org/xxxxxx

## ARTICLE TYPE

**Scheme 1** Schematic diagram showing the principle of colorimetric detection of arsenic ions using aptamer-functionalized silver nanoparticles.

**Table 1** Coded and actual levels for independent factors used in the experimental design.

**Table 2** Comparison between the proposed aptasensor for sensing of As (III) and other reported aptasensors for the sensing of heavy metal ions.

**Table 3** Central composite rotatable quadratic polynomial model, experimental data, and actual and predicted values for response surface analysis

**Tables 4** Analysis of variance (ANOVA) of the response surface quadratic model for the colorimetric detection of As (III).

<sup>a</sup> DF—degrees of freedom.  $R^2=97.01\%$  Adj.  $R^2=94.33\%$  Adeq Precision=22.209

**Table 5** Analytical results using proposed sensor for As(III) in water samples.

1 **Fig. 1.** The UV–Vis spectra of (a) SNPs, (b) Atp-SNPs and (c) Atp-SNPs in the presence of  $700 \mu\text{g L}^{-1}$  As (III) ions in  
2 aqueous media.

3 **Fig. 2.** TEM image of the prepared (a) Apt-SNPs, (b) Atp-SNPs in the presence of  $700 \mu\text{g L}^{-1}$  As (III) ions in aqueous  
4 media.

5 **Fig. 3.** Optimal incubation time for preparation of Apt-SNPs for sensing  $150 \mu\text{g L}^{-1}$  of As (III) in aqueous media.

6 **Fig. 4.** Effect of (a) pH and (b) time on the stability of synthesized Apt-SNPs.

7 **Fig. 5.** (A) Absorbance spectra for optimization of aptamer concentration ( $0.5, 1, 5$  and  $10 \text{ mg L}^{-1}$ ) for sensing  $0.1 \text{ mg L}^{-1}$  of  
8 As (III) in aqueous media.

9 **Fig. 6.** (A) The UV–Vis absorbance spectra of Apt-SNPs aggregate solution over the As (III) concentration of  $0.05\text{--}0.7 \text{ mg}$   
10  $\text{L}^{-1}$ , (B) the peak absorbance change at  $403 \text{ nm}$  as a function of As (III) concentration.

11 **Fig. 7.** Specificity assays. (A) The UV–Vis spectra of Apt-SNPs solution in the presence of different ions with various  
12 concentrations (a)  $0 \text{ mg L}^{-1}$  As (III), (b-h)  $350 \mu\text{g L}^{-1}$   $\text{Na}^+$ ,  $\text{Ca}^{2+}$ ,  $\text{Cd}^{2+}$ ,  $\text{Pb}^{2+}$ ,  $\text{Sb}^{3+}$ ,  $\text{Bi}^{3+}$  and  $\text{As}^{5+}$  respectively, (i)  $350 \mu\text{g L}^{-1}$   
13 As (III). (B) The relative response of the sensing system to different ions. The relative signal changes for other  
14 interferences, compared to As (III), are very small, indicating excellent selectivity.

15 **Fig. 8.** Plot of measured and model predicted values of the response variable.

16 **Fig. 9.** The response surface plots (left) and their corresponding contour plots (right) showing effect of (a) conjugation time  
17 and aptamer concentration, (b) pH and aptamer concentration, (c) pH and conjugation time on colorimetric As (III)  
18 detection by proposed aptasensor  
19

20  
21  
22  
23  
24  
25  
26  
27  
28  
29  
30  
31  
32  
33  
34  
35  
36  
37  
38  
39  
40  
41  
42  
43  
44  
45  
46  
47  
48  
49  
50  
51  
52  
53  
54  
55  
56  
57  
58  
59  
60

Table 1

Factors	Unit	Coded values				
		$-\alpha$	-1	+1	$+\alpha$	
		Actual levels				
Aptamer concentration (A)	mg L <sup>-1</sup>	0.02	0.05	0.1	0.15	0.18
Conjugation time (B)		7.00	10.00	15.00	20.00	23.41
pH (C)		3.64	5.00	7.00	9.00	10.36

**Table 2**

<b>Probe</b>	<b>Detection</b>	<b>Target</b>	<b>LOD</b>	<b>Ref</b>
<b>Apt-Au NPs</b>	Colorimetric	Hg <sup>2+</sup>	0.0201 mg L <sup>-1</sup>	18
<b>Apt-Au NPs</b>	Colorimetric	K <sup>+</sup>	39.10 mg L <sup>-1</sup>	19
<b>Apt-Au NPs &amp; DNAzyme</b>	Colorimetric	Pb <sup>2+</sup>	0.025 mg L <sup>-1</sup>	20
<b>Apt-Au NPs &amp; DNAzyme</b>	Colorimetric	Pb <sup>2+</sup>	0.083 mg L <sup>-1</sup>	25
<b>DNA-AuNPs</b>	Fluorescence detection	Hg <sup>2+</sup>	~0.010 mg L <sup>-1</sup>	26
<b>Au NPs &amp; Dye-Apt</b>	Fluorescence detection	Hg <sup>2+</sup>	0.008 mg L <sup>-1</sup>	27
<b>DNA-AuNPs</b>	Fluorescence detection	Pb <sup>2+</sup> and Hg <sup>2+</sup>	0.0265 mg L <sup>-1</sup> and 0.0243 mg L <sup>-1</sup>	28
<b>Apt-Ag NPs</b>	Colorimetric	As <sup>3+</sup>	0.006 mg L <sup>-1</sup>	This work

Table 3

Run	Real variables			Observed	Predicted	Residual value
	A: aptamer concentration	B: onjugation time	C:pH			
1	0.00	0.00	-1.68	0.468	0.484	0.016
2	0.00	-1.68	0.00	0.412	0.443	0.031
3	-1.68	0.00	0.00	0.453	0.476	0.023
4	0.00	0.00	0.00	0.421	0.438	0.017
5	1.00	-1.00	-1.00	0.584	0.607	0.023
6	0.00	0.00	0.00	0.566	0.583	0.017
7	0.00	1.68	0.00	0.586	0.595	0.009
8	1.00	1.00	1.00	0.551	0.574	0.023
9	0.00	0.00	1.68	0.687	0.664	-0.023
10	0.00	0.00	0.00	0.645	0.612	-0.033
11	-1.00	1.00	-1.00	0.681	0.648	-0.033
12	1.00	1.00	-1.00	0.657	0.634	-0.023
13	-1.00	-1.00	1.00	0.242	0.210	-0.032
14	0.00	0.00	0.00	0.451	0.428	-0.023
15	-1.00	1.00	1.00	0.664	0.660	-0.004
16	1.00	-1.00	1.00	0.658	0.660	0.002
17	0.00	0.00	0.00	0.649	0.660	0.011
18	1.68	0.00	0.00	0.661	0.660	-0.001
19	0.00	0.00	0.00	0.662	0.660	-0.002
20	-1.00	-1.00	-1.00	0.659	0.660	0.001

Table 4

Source	Sum of squares	DF <sup>a</sup>	Mean sum of squares	F-value	p-value
<b>Model</b>	0.2721	9	0.0302	36.0927	< 0.0001
<b>A</b>	0.0033	1	0.0033	3.9159	0.0760
<b>B</b>	0.0003	1	0.0003	0.3081	0.5911
<b>C</b>	0.0573	1	0.0573	68.3970	< 0.0001
<b>A<sup>2</sup></b>	0.0009	1	0.0009	1.0720	0.3249
<b>B<sup>2</sup></b>	0.0007	1	0.0007	0.8032	0.3912
<b>C<sup>2</sup></b>	0.2105	1	0.2105	251.3139	< 0.0001
<b>AB</b>	6.13E-06	1	6.13E-06	0.0073	0.9335
<b>AC</b>	0.0002	1	0.0002	0.1828	0.6780
<b>BC</b>	6.13E-06	1	6.13E-06	0.0073	0.9335
<b>Lack of fit</b>	0.0082	5	0.0017	59.3266	0.0002
<b>Total</b>	0.2804	19			

**Table 5**

Sample	Added	GF-AAS	UV-Vis	Recovery (%)
Tap water ( $\mu\text{g L}^{-1}$ )	50	50.1	50.0	96.8
River water ( $\mu\text{g L}^{-1}$ )	95	99.8	93.5	93.7
Well water ( $\mu\text{g L}^{-1}$ )	690	694.8	669.2	96.3

Scheme 1

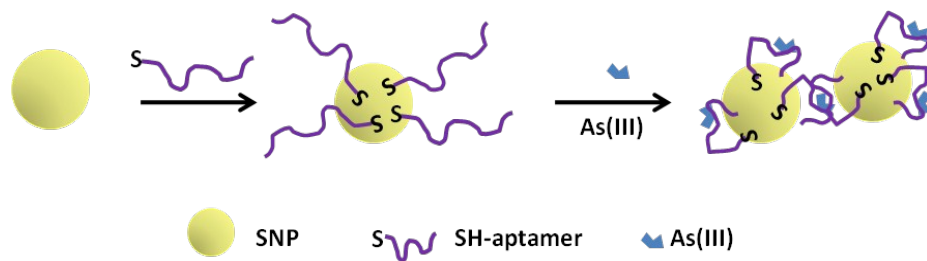


Fig. 1.

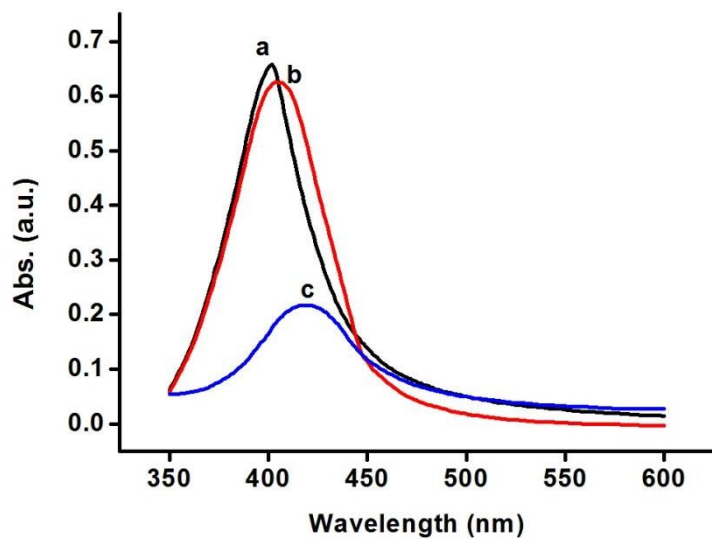


Fig. 2.

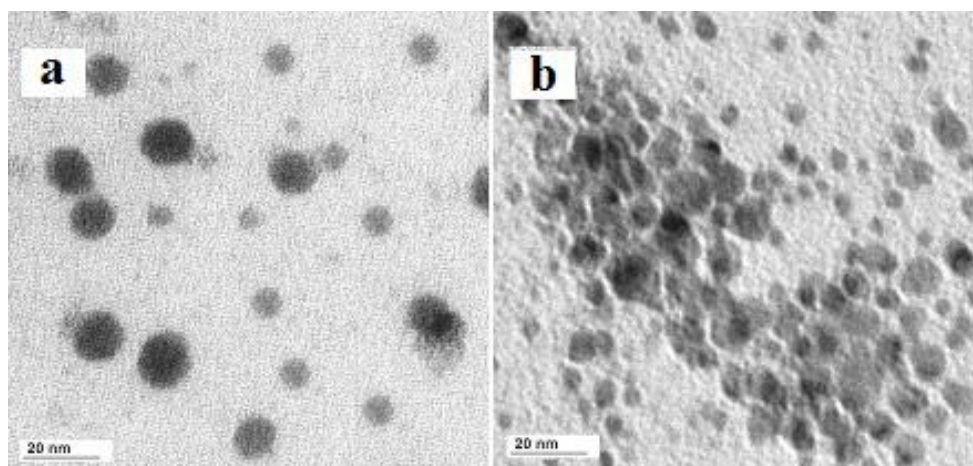


Fig.3.

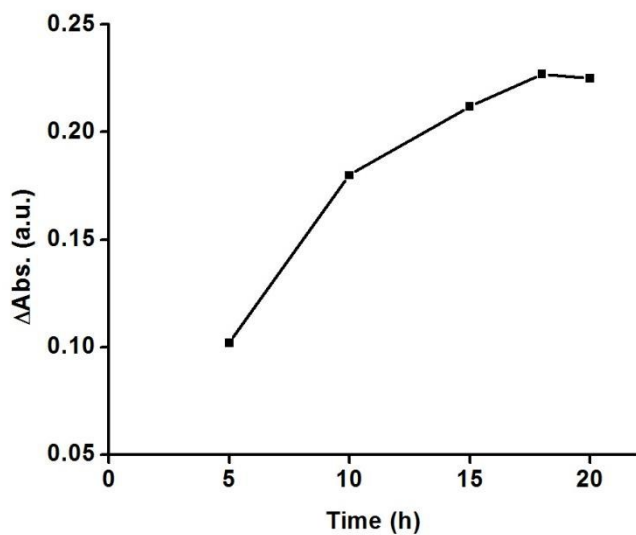


Fig.4.

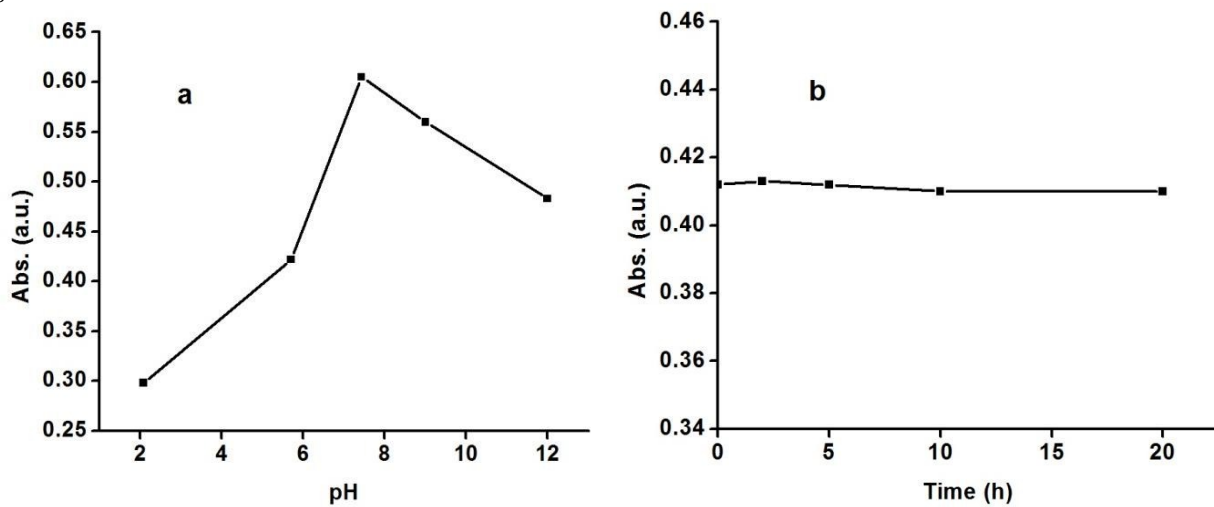


Fig.5.

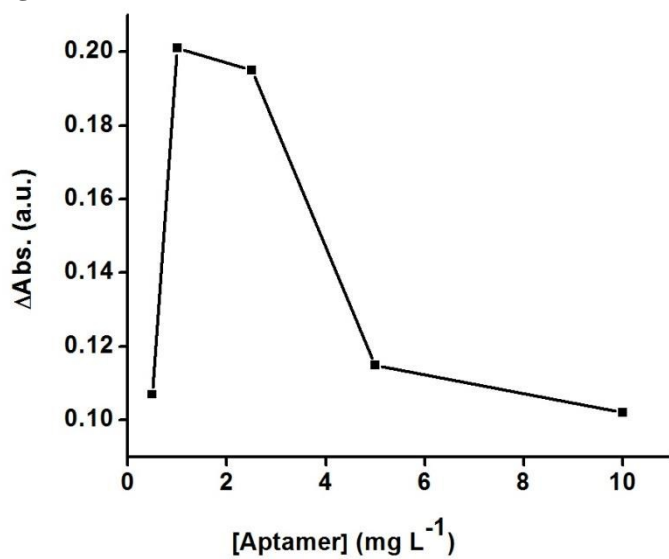


Fig.6.

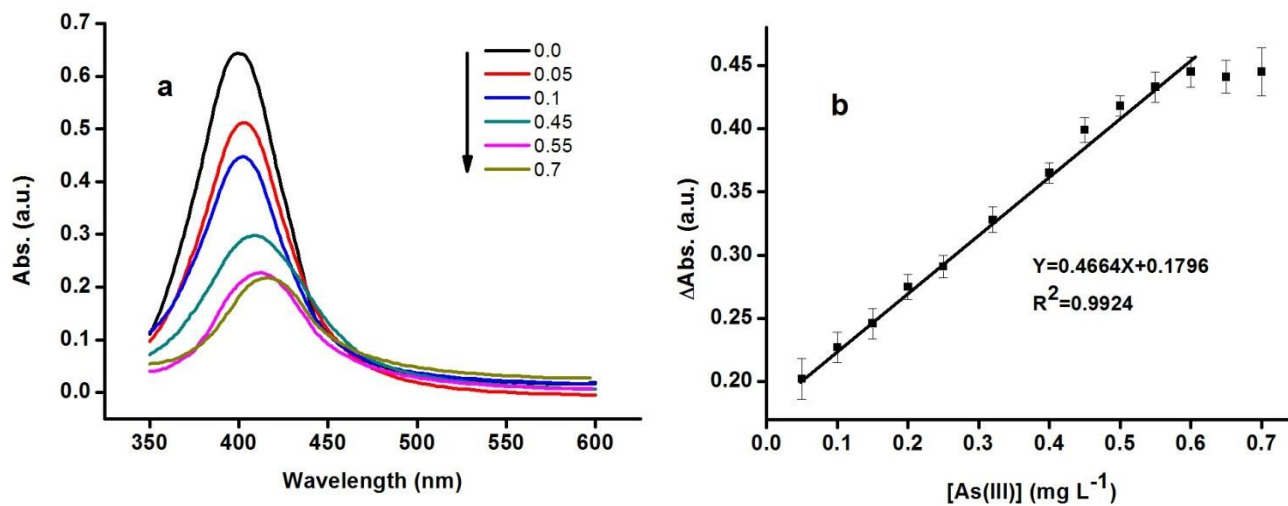
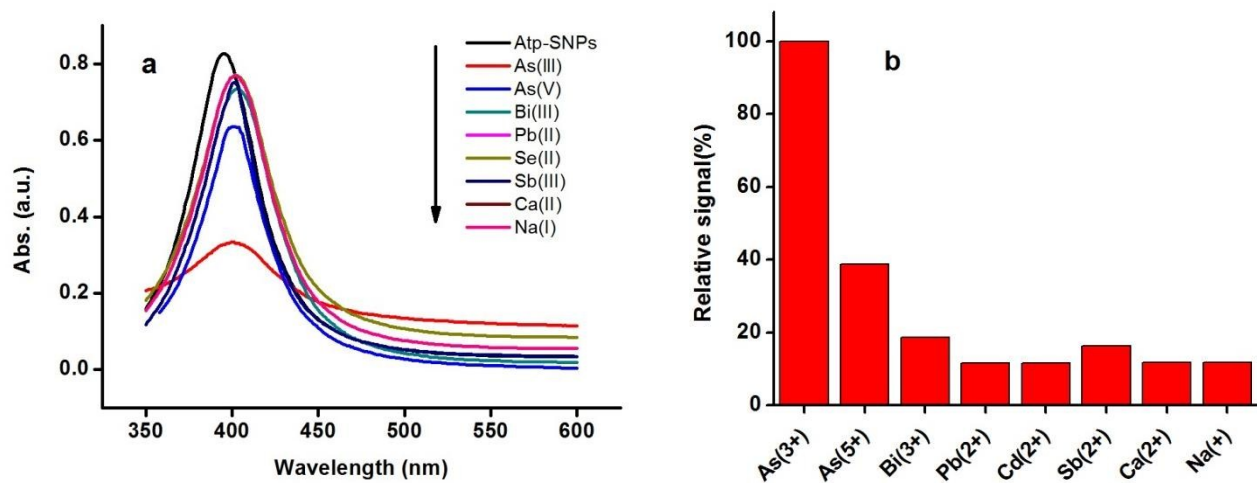


Fig.7.



5

Fig.8.

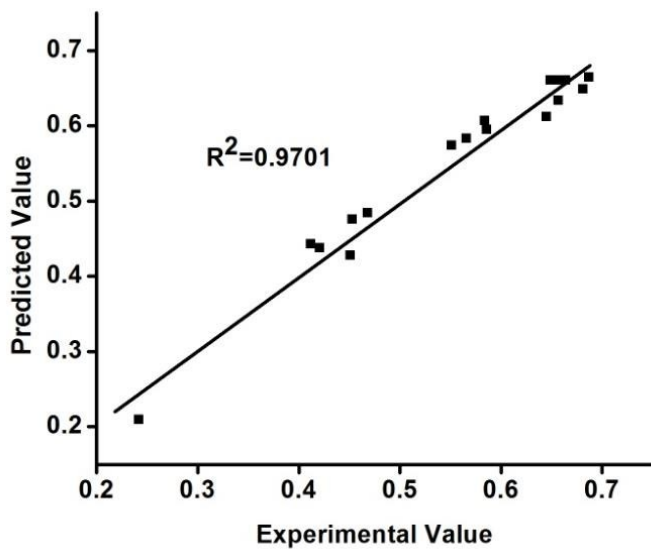


Fig.9.

